A sample slide

Microscopic simulation of superconductor-topological insulator proximity structures

Mahmoud Lababidi, Erhai Zhao
George Mason University

March 4, 2011

Abstract

We present microscopic, self-consistent calculations of the superconducting order parameter and pairing correlations near the interface of an *s*-wave superconductor and a three-dimensional topological insulator with spin-orbit coupling. We discuss the suppression of the order parameter by the topological insulator and show that the equal-time pair correlation functions in the triplet channel, induced by spin-flip scattering at the interface, are of $p_x \pm ip_y$ symmetry. We verify that the spectrum at sub-gap energies is well described by the Fu-Kane model. The sub-gap modes are viewed as interface states with spectral weight penetrating well into the superconductor. We extract the phenomenological parameters of the Fu-Kane model from microscopic calculations, and find they are strongly renormalized from the bulk material parameters. This is consistent with previous results of Stanescu et al for a lattice model using perturbation theory in the tunneling limit.

Outline

Fu-Kane Model

PRL **100,** 096407 (2008) PHYSICAL REVIEW LETTERS week ending 7 MARCH 2008

Superconducting Proximity Effect and Majorana Fermions at the Surface of a Topological Insulator

Liang Fu and C. L. Kane

Department of Physics and Astronomy, University of Pennsylvania, Philadelphia, Pennsylvania 19104, USA

(Received 11 July 2007; published 6 March 2008)

We study the proximity effect between an s-wave superconductor and the surface states of a strong topological insulator. The resulting two-dimensional state resembles a spinless $p_x + ip_y$ superconductor, but does not break time reversal symmetry. This state supports Majorana bound states at vortices. We show that linear junctions between superconductors mediated by the topological insulator form a nonchiral one-dimensional wire for Majorana fermions, and that circuits formed from these junctions provide a method for creating, manipulating, and fusing Majorana bound states.

DOI: 10.1103/PhysRevLett.100.096407 PACS numbers: 71.10.Pm, 03.67.Lx, 74.45.+c, 74.90.+n

Fu-Kane Model

$$H_{FK}(\mathbf{k}) = \begin{pmatrix} h_s(\mathbf{k}) & i\sigma_y\Delta_s \\ -i\sigma_y\Delta_s^* & -h_s^*(-\mathbf{k}) \end{pmatrix}, \tag{1}$$

$$h_s(\mathbf{k}) = -\mu_s + v_s(\sigma_x k_y - \sigma_y k_x), \tag{2}$$

$$\mathbf{k} = (k_x, k_y), \tag{3}$$

L. Fu and C. L. Kane, Phys. Rev. Lett. 100, 096407 (2008)

Geometry

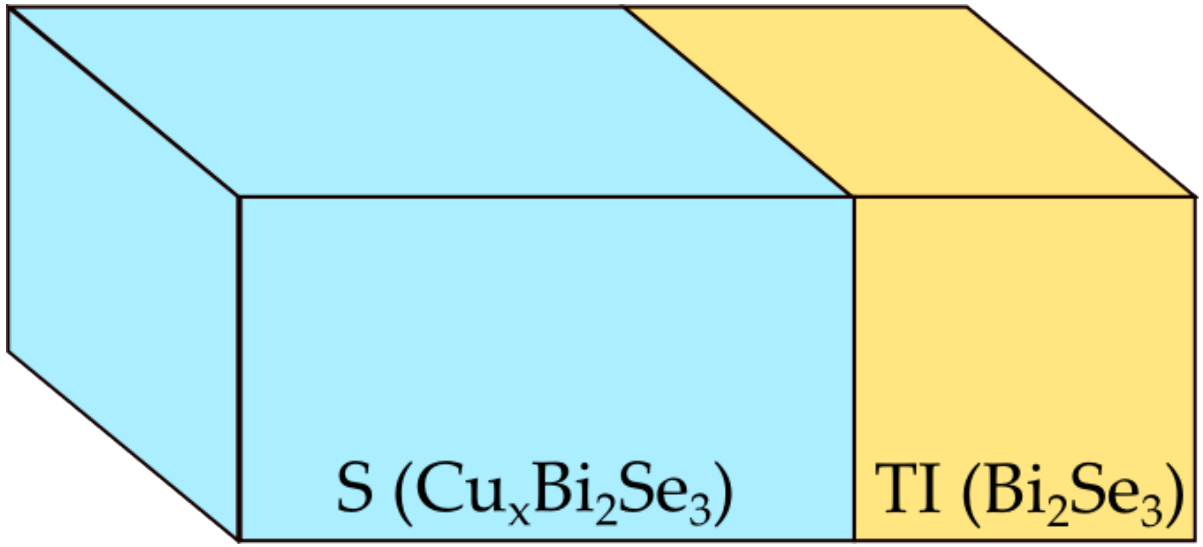

This model is inspired partly by superconductor $Cu_xBi_2Se_3$. The transition temperature at optimal doping $x = 0.12$ is $T_c = 3.8$K, which corresponds to a zero temperature superconducting gap $\Delta \sim 0.6$meV [**cu1**, **cu2**]. The Fermi level is 0.25eV above the bottom of the conduction band, and the Fermi wave vector $k_f \sim 0.12\text{Å}^{-1}$. The pairing symmetry of $Cu_xBi_2Se_3$ is to our best knowledge not clear at present. If it turns out to be a conventional s-wave superconductor, its mains features will be captured by H_S above with suitable choice of E_f and Δ.

Band Diagram

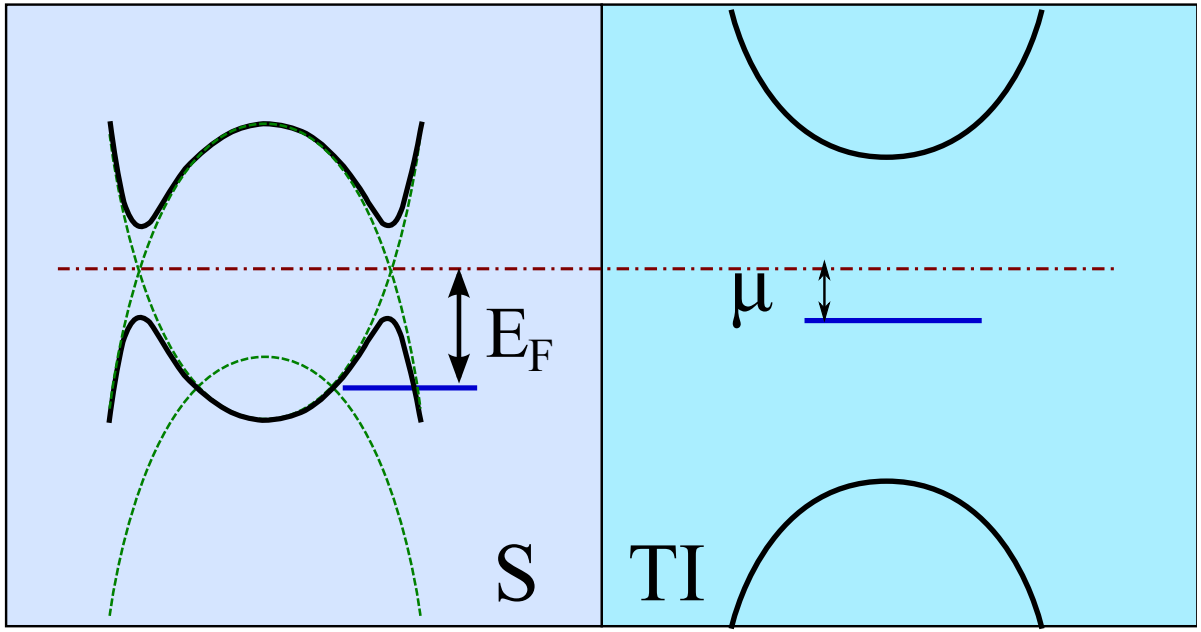

Figure: Schematic (not to scale) band diagrams in a superconductor-topological insulator (S-TI) proximity structure. E_f is the Fermi energy of the metal described by H_M measured from the band crossing point. μ is the chemical potential of TI measured from the band gap center. The superconducting gap is much smaller than the band gap of TI.

Model and Basic equations

low energy effective $\mathbf{k}\cdot\mathbf{p}$ $\mathcal{H}$ in basis $\{|1\uparrow\rangle, |1\downarrow\rangle, |2\uparrow\rangle, |2\downarrow\rangle\}$,

$$H_{TI}(\mathbf{k}) = \begin{pmatrix} M(\mathbf{k}) & 0 & A_1 k_z & A_2 k_- \\ 0 & M(\mathbf{k}) & A_2 k_+ & -A_1 k_z \\ A_1 k_z & A_2 k_- & -M(\mathbf{k}) & 0 \\ A_2 k_+ & -A_1 k_z & 0 & -M(\mathbf{k}) \end{pmatrix} - \mu \hat{I}. \qquad (4)$$

Here $k_\pm = k_x \pm i k_y$,
$M(\mathbf{k}) = M - B_1 k_z^2 - B_2(k_x^2 + k_y^2)$,
and $\hat{I}$ is 4×4 unit matrix.
$M = 0.28$ eV, $A_1 = 2.2$ eVÅ, $A_2 = 4.1$ eVÅ, $B_1 = 10$ eVÅ^2,
$B_2 = 56.6$ eVÅ^2. We work
μ as a tuning parameter.
H. Zhang et al, Nature Physics 5, 438 (2009)

($A_1 = A_2 = 0$) Here Δ is the superconducting order parameter, $\psi^\dagger_{l\sigma}$ is the electron creation operator for orbital $l = 1, 2$ and spin $\sigma = \uparrow, \downarrow$.

A sample slide

Here $h_0(\mathbf{k}_\parallel, \partial_z) = M - B_1\partial_z^2 - B_2 k_\parallel^2$, $\mu(z)$ and $A_i(z)$ are piece-wise constant,

$$\mu(z) = E_f\theta(d-z) + \mu\theta(z-d), \tag{5}$$

$$A_i(z) = A_i\theta(z-d), \quad i = 1,2 \tag{6}$$

in terms of the step function θ. The order parameter obeys the gap equation

$$\Delta(z) = g(z)\int d\mathbf{k}_\parallel \langle \psi_{2\uparrow}(\mathbf{k}_\parallel, z)\psi_{2\downarrow}(-\mathbf{k}_\parallel, z)\rangle. \tag{7}$$

We assume $g(z) = g\theta(d-z)$, the coupling constant g determines the bulk gap.

A sample slide

To self-consistently solve Eq. (**??**) and (7), we introduce Bogoliubov transformation

$$\psi_{l\sigma}(\mathbf{k}_{\parallel}, z) = \sum_{n} u_{n,l\sigma}(\mathbf{k}_{\parallel}, z)\gamma_{n,\mathbf{k}_{\parallel}} + v^{*}_{n,l\sigma}(\mathbf{k}_{\parallel}, z)\gamma^{\dagger}_{n,\mathbf{k}_{\parallel}} \tag{8}$$

to diagonalize $\mathcal{H}$ as

$$\mathcal{H} = E_g + \int d\mathbf{k}_{\parallel} \sum_{n} \epsilon_n(k_{\parallel})\gamma^{\dagger}_{n,\mathbf{k}_{\parallel}}\gamma_{n,\mathbf{k}_{\parallel}}, \tag{9}$$

where E_g is the ground state energy, and $\gamma^{\dagger}_{n,\mathbf{k}_{\parallel}}$ is the creation operator of Bogoliubov quasiparticles with energy $\epsilon_n(k_{\parallel})$.

A sample slide

The wave function u and v satisfy the following Bogliubov-de Gennes (BdG) equation,

$$\hat{H}_B(\mathbf{k}_\parallel, z)\hat{\phi}_n(\mathbf{k}_\parallel, z) = \epsilon_n(k_\parallel)\hat{\phi}_n(\mathbf{k}_\parallel, z). \tag{10}$$

Here, the BdG Hamiltonian

$$\hat{H}_B = \begin{pmatrix} h_0 - \mu & \mathbf{d}\cdot\boldsymbol{\sigma} & 0 & 0 \\ \mathbf{d}\cdot\boldsymbol{\sigma} & -h_0 - \mu & 0 & -\Delta\, i\sigma_y \\ 0 & 0 & \mu - h_0 & \mathbf{d}\cdot\boldsymbol{\sigma}^* \\ 0 & \Delta^*\, i\sigma_y & \mathbf{d}\cdot\boldsymbol{\sigma}^* & \mu + h_0 \end{pmatrix}, \tag{11}$$

A sample slide

and the wave function (dropping the arguments)

$$\hat{\phi}_n = (u_{n,1\uparrow}, u_{n,1\downarrow}, u_{n,2\uparrow}, u_{n,2\downarrow}, v_{n,1\uparrow}, v_{n,1\downarrow}, v_{n,2\uparrow}, v_{n,2\downarrow})^{\mathrm{T}}. \quad (12)$$

The vector $\mathbf{d}(\mathbf{k}_{\|}, z)$ is defined as

$$d_x = A_1(z)k_x, \;\; d_y = A_1(z)k_y, \;\; d_z = A_2(z)(-i\partial_z). \quad (13)$$

Other quantities such as $h_0(\mathbf{k}_{\|}, z)$, $\mu(z)$, and $\Delta(z)$ are defined above. In terms of the wave functions, the zero temperature gap equation becomes

$$\Delta(z) = g(z) \int d\mathbf{k}_{\|} \sum_{n}^{0<\epsilon_n<\omega_D} u_{n,2\uparrow}(\mathbf{k}_{\|}, z) v^*_{n,2\downarrow}(-\mathbf{k}_{\|}, z), \quad (14)$$

where the summation denoted by prime is restricted to $\epsilon_n < \omega_D$ with ω_D being the Debye frequency.

A sample slide

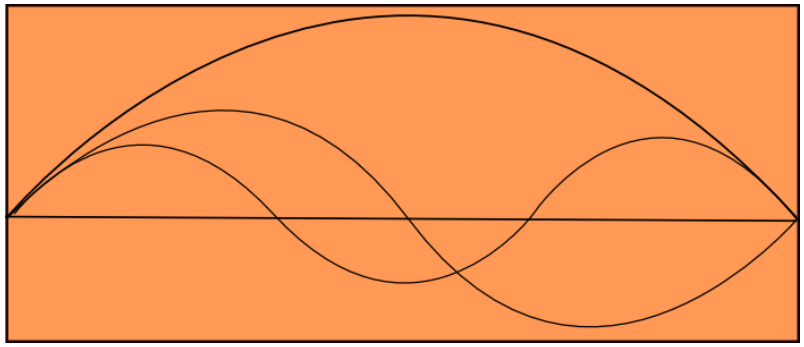

$$u_{n,l\sigma}(z) = \sum_m u_{nm}^{l\sigma}\,\phi_m(z), \quad v_{n,l\sigma}(z) = \sum_m v_{nm}^{l\sigma}\,\phi_m(z), \tag{15}$$

$$\Delta(z) = \sum_m \Delta_m\,\phi_m(z), \quad \phi_m(z) = \sqrt{2/L}\sin(k_m z). \tag{16}$$

The integer $m = 1, 2, ..., N$ labels the quantized z momentum $k_m = m\pi/L$. The cutoff N is chosen as

$$B_1 k_N^2 = B_1(N\pi/L)^2 = M + E_f + \omega_D. \tag{17}$$

BdG equation becomes an $8N \times 8N$ matrix equation.

.

K. Halterman and O. T. Valls, Phys. Rev. B 65, 014509 (2001)
B. P. Stojkovic and O. T. Valls, Phys. Rev. B 47, 5922 (1993)

A sample slide

To analyze the spectrum of the system, it is convenient to define the retarded Green's function

$$G^R_{l\sigma}(\mathbf{k}_\parallel, z, t) = -i\theta(t)\langle\{\psi_{l\sigma}(\mathbf{k}_\parallel, z, t), \psi^\dagger_{l\sigma}(\mathbf{k}_\parallel, z, 0)\}\rangle \tag{18}$$

where the time-dependent field operators are in Heisenberg picture. For given $\mathbf{k}_\parallel$ and z, the spectral functions are defined as

$$N_{l\sigma}(\mathbf{k}_\parallel, z, \omega) = -\mathrm{Im}\, G^R_{l\sigma}(\mathbf{k}_\parallel, z, \omega), \tag{19}$$

$$N(\mathbf{k}_\parallel, z, \omega) = \sum_{l\sigma} N_{l\sigma}(\mathbf{k}_\parallel, z, \omega). \tag{20}$$

In terms of the wave functions and eigen energies,

$$N_{l\sigma}(\mathbf{k}_\parallel, z, \omega > 0) = \sum_n |u_{n,l\sigma}(\mathbf{k}_\parallel, z)|^2 \delta(\omega - \epsilon_n). \tag{21}$$

We also introduce the equal-time pair correlation functions for the conduction electrons

$$F_{\alpha\beta}(\mathbf{k}_\parallel, z) = \langle\psi_{2\alpha}(\mathbf{k}_\parallel, z)\psi_{2\beta}(-\mathbf{k}_\parallel, z)\rangle. \tag{22}$$

For example, at zero temperature we have

Order Parameter Δ

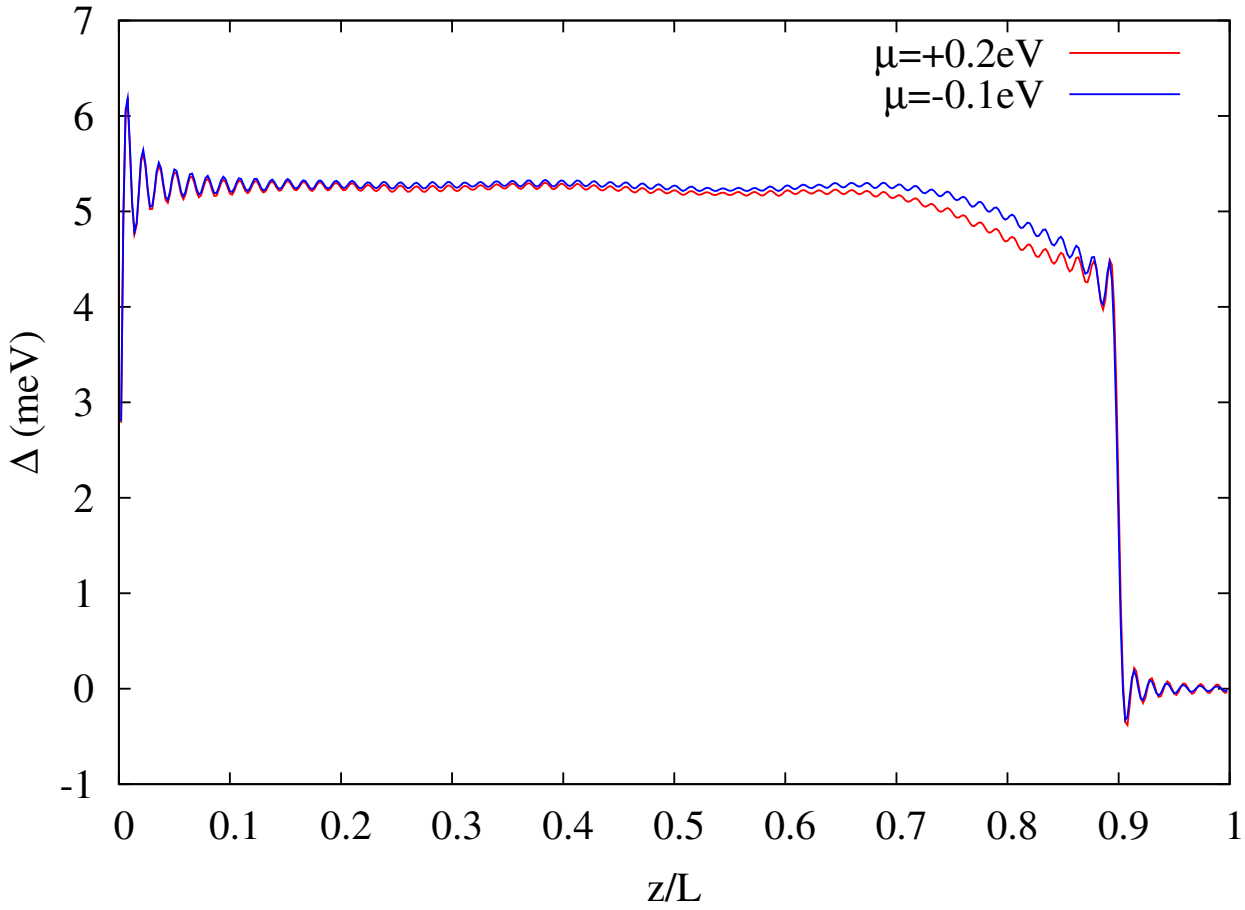

Figure: The order parameter profile for two different chemical potentials of the topological insulator, $\mu = -0.1$eV and $\mu = 0.2$eV. $L = 160$nm, $\Delta_0 \sim 5.2$meV.

A sample slide

$$E(k) = \sqrt{|\Delta_s|^2 + (v_s k \pm \mu_s)^2}. \tag{25}$$

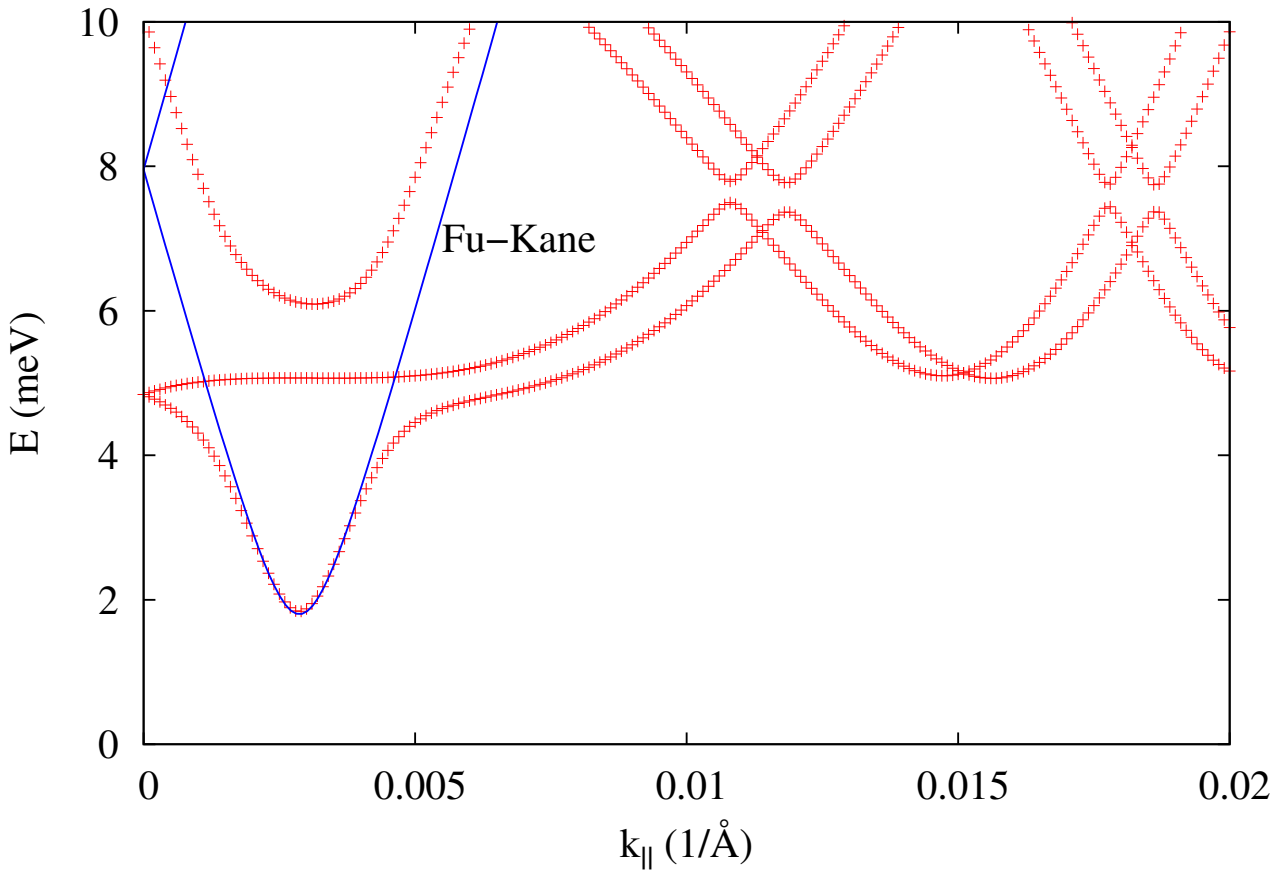

Figure: The lowest few energy levels $\epsilon_n(k_{||})$. $\mu = 0$, $L = 160$nm, and the bulk superconducting gap $\Delta_0 \sim 5.2$meV. A well-defined interface mode is

A sample slide

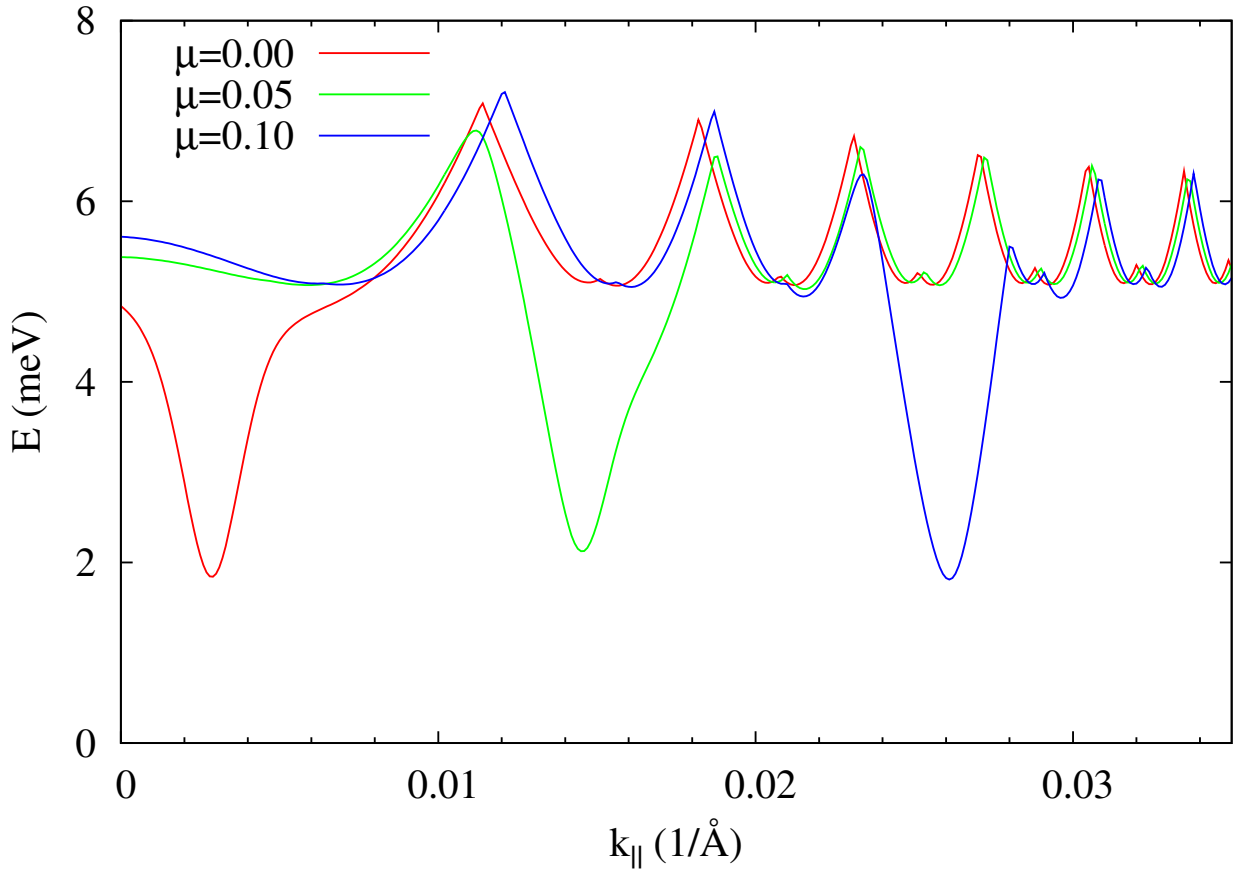

Figure: The dispersion of the lowest energy level for different μ (in eV). Other parameters are the same as in Fig. 3, $L = 160$nm and $\Delta_0 \sim 5.2$meV. Fu-Kane model well describes the lowest energy mode. As μ is increased, Δ_s and v_s stay roughly the same, while μ_s scales linearly with μ.

A sample slide

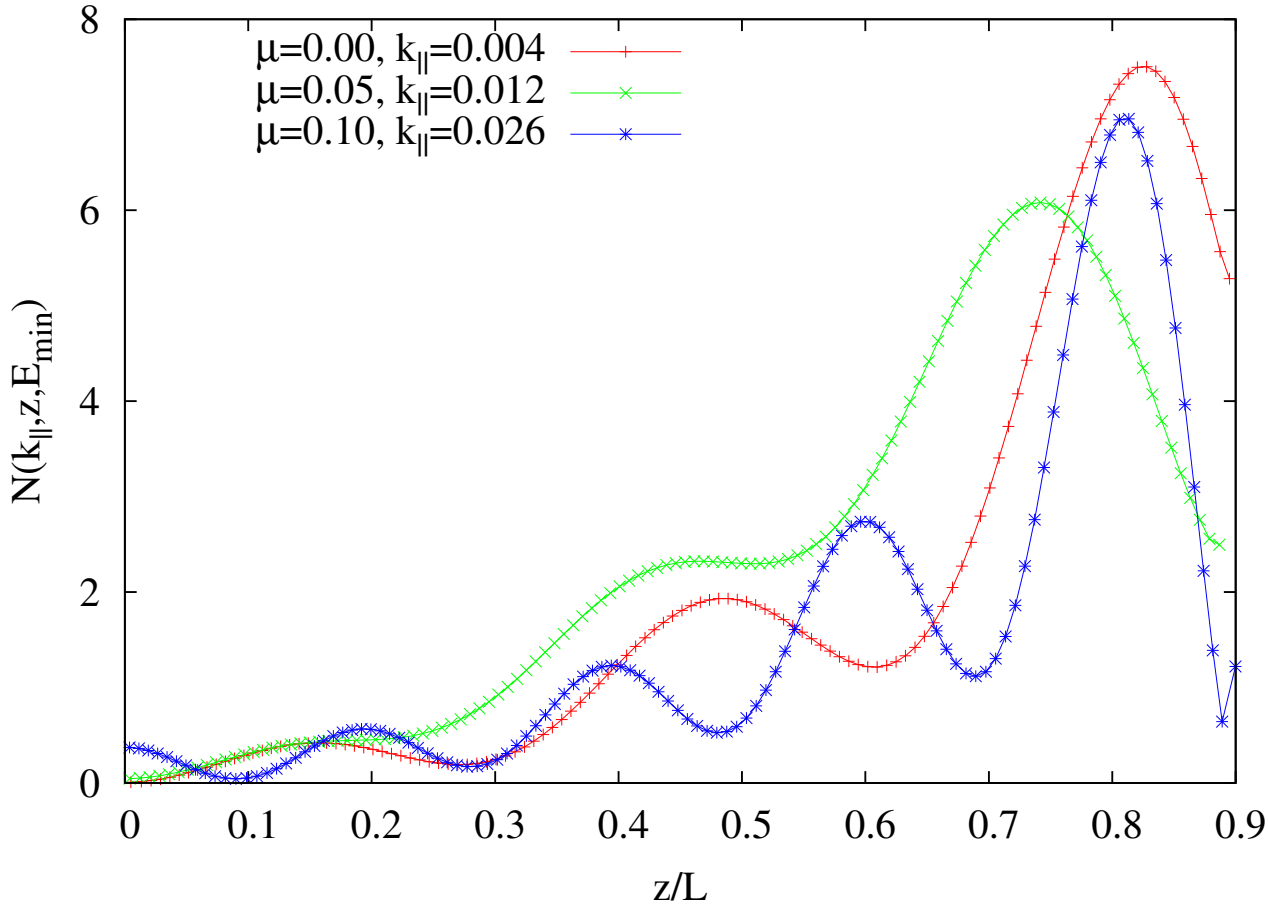

Figure: The spectral function $N(k_{\|}, z, \omega)$ of the lowest energy level, $\omega = E_{min}$, shown in Fig. 4. The interface is at $z = 0.9L$, L=160nm. The spectral function oscillates rapidly with z, so only its envelope is plotted.

A sample slide

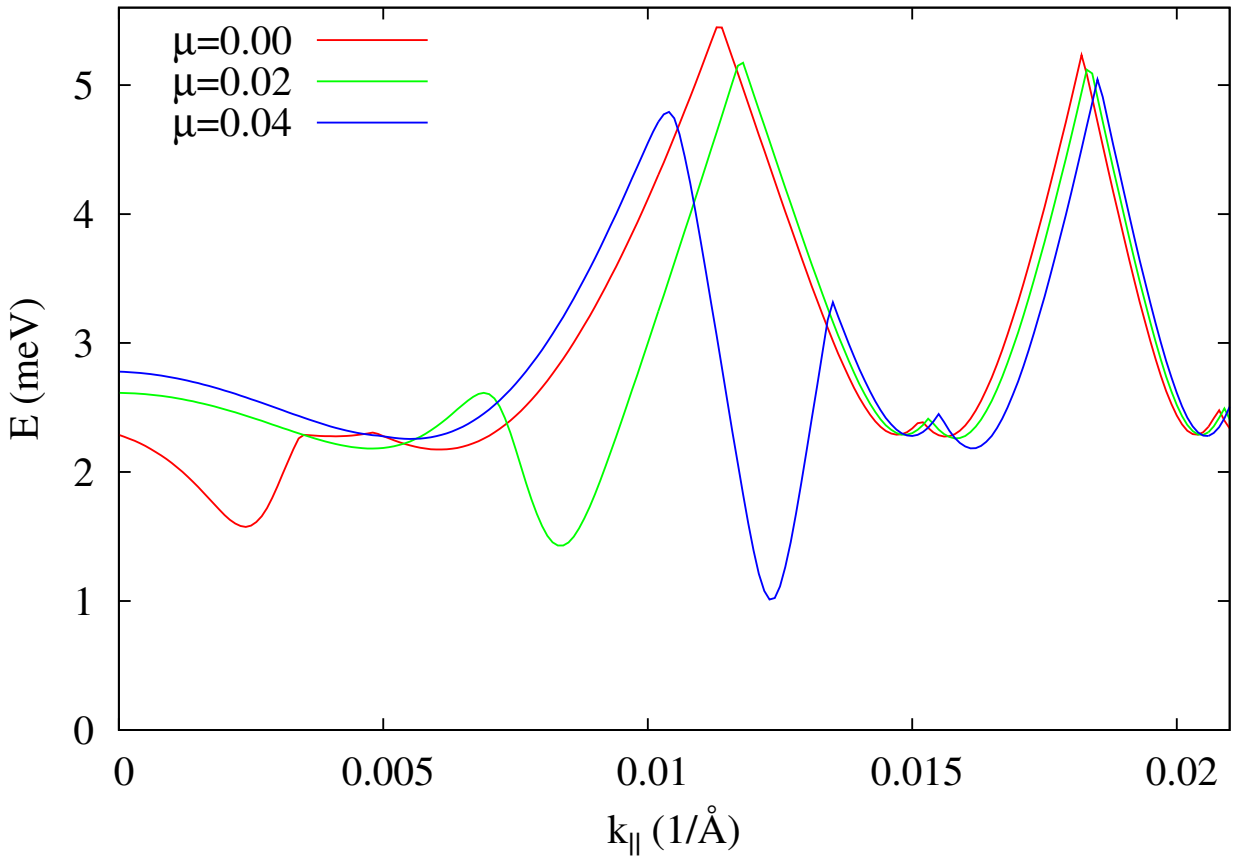

Figure: The lowest energy level of an S-TI structure with $L = 160$nm, $d = 0.9L$, $\Delta_0 = 2.4$meV. μ is the chemical potential of the TI and measured in eV.

Triplet Pair Correlations

Using these relations, we find

$$F_{\uparrow\uparrow}(\mathbf{k}_{\parallel}, z) = F_{\uparrow\uparrow}(k_{\parallel}, z)e^{-i\varphi_k}, \tag{26}$$

$$F_{\downarrow\downarrow}(\mathbf{k}_{\parallel}, z) = F_{\downarrow\downarrow}(k_{\parallel}, z)e^{+i\varphi_k}. \tag{27}$$

Namely $F_{\uparrow\uparrow}$ ($F_{\downarrow\downarrow}$) has $p_x - ip_y$ ($p_x + ip_y$) orbital symmetry. Finally, the remaining triplet correlation function

$$\langle \psi_{2\uparrow}(\mathbf{k}_{\parallel}, z)\psi_{2\downarrow}(-\mathbf{k}_{\parallel}, z) + \psi_{2\downarrow}(\mathbf{k}_{\parallel}, z)\psi_{2\uparrow}(-\mathbf{k}_{\parallel}, z)\rangle = 0 \tag{28}$$

A sample slide

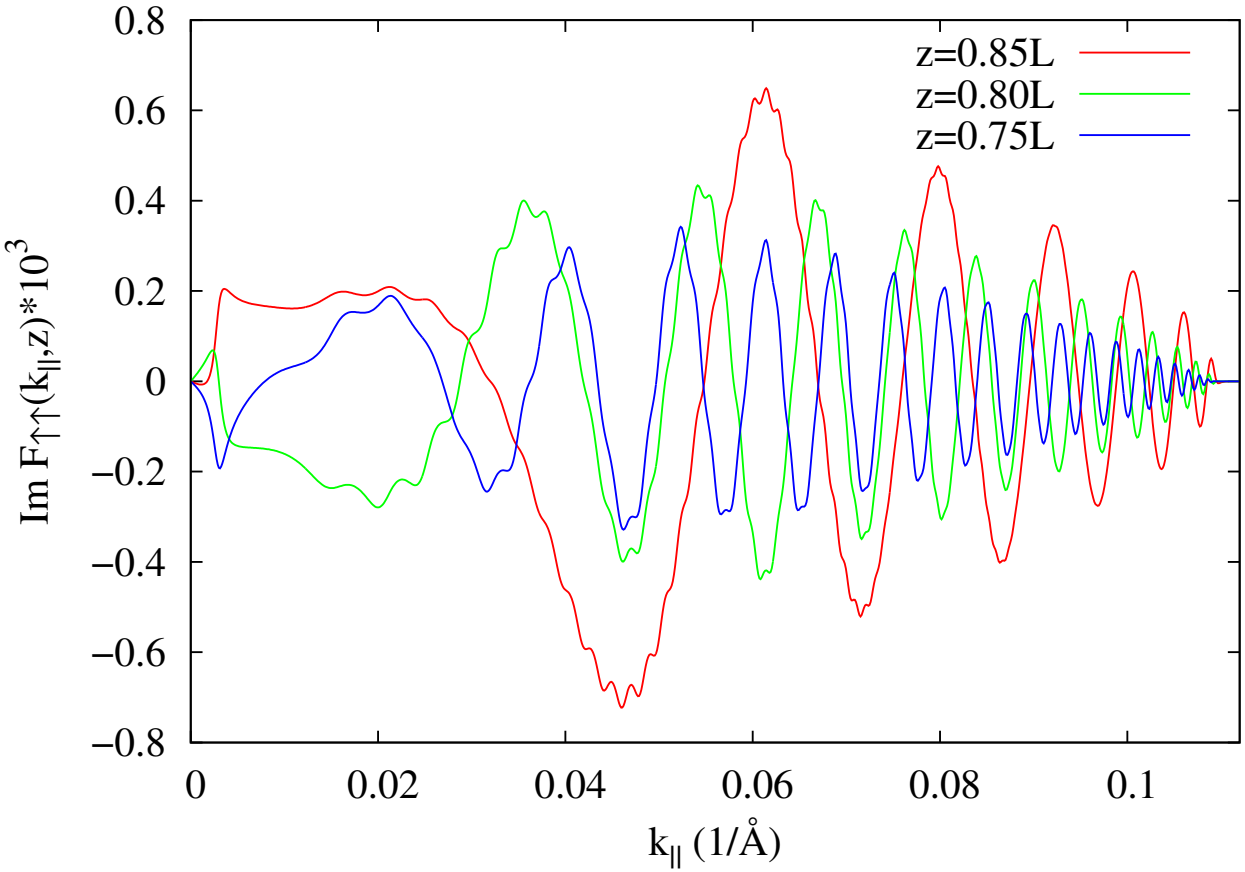

Figure: The imaginary part of triplet pair correlation function $F_{\uparrow\uparrow}(k_{\|}, z)$. The S-TI interface is at $d = 0.9L$. $\mu = 0$, $L = 160$nm, $\Delta_0 = 5.2$meV.

A sample slide

We find that $F_{\uparrow\uparrow}(k_{\parallel}, z)$ is purely imaginary and identical to $F_{\downarrow\downarrow}(k_{\parallel}, z)$. The results for $\mu = 0$, $L = 160\text{nm}$, $d = 0.9L$, $\Delta_0 = 5.2\text{meV}$ are plotted in Fig. 7. $F_{\uparrow\uparrow}$ vanishes at $k_{\parallel} = 0$ as well as for large $k_{\parallel}$, namely when $k_{\parallel} > \sqrt{(E_F + \omega_D + M)/B_2}$. This is consistent with lack of pairing in both limits. The behavior of $F_{\uparrow\uparrow}$ for small $k_{\parallel}$ is illustrated in Fig. 8 for $\mu = 0$, $L = 300\text{nm}$, $d = 0.95L$, $\Delta_0 = 0.6\text{meV}$. As comparison, we also plotted the singlet pair correlation function

$$F_{\uparrow\downarrow}(\mathbf{k}_{\parallel}, z) = \sum_{n}{}' u_{n,2\uparrow}(\mathbf{k}_{\parallel}, z) v^{*}_{n,2\downarrow}(-\mathbf{k}_{\parallel}, z) \tag{29}$$

which is s-wave and purely real.

A sample slide

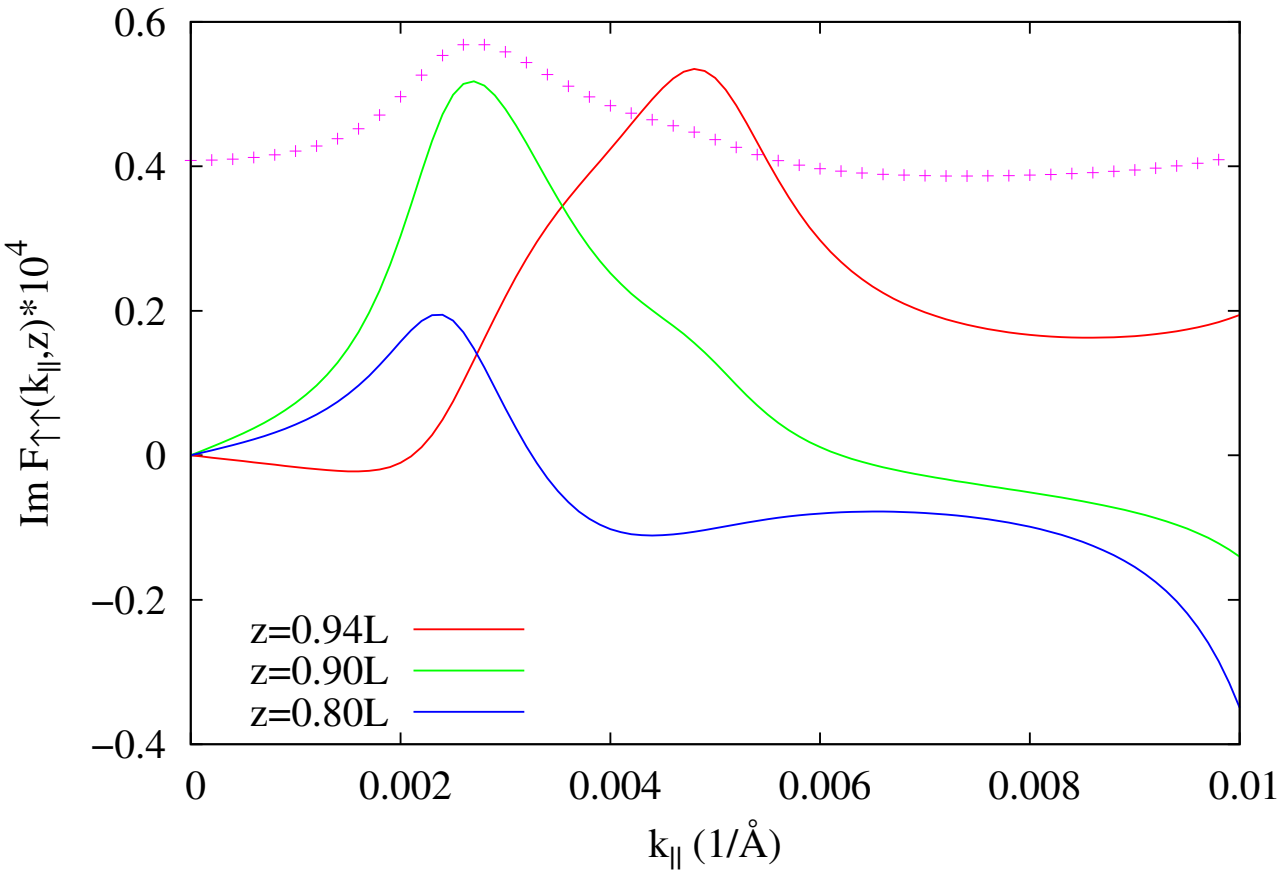

Figure: The imaginary part of $F_{\uparrow\uparrow}(k_{\|}, z)$. $\mu = 0$, $L = 300$nm, $d = 0.95L$, $\Delta_0 = 0.6$meV. As comparison, the data points show the singlet pair correlation function $F_{\uparrow\downarrow}(k_{\|}, z = 0.9L)/3$.

A sample slide

In summary, we have investigated the proximity effect between an *s*-wave superconductor and a topological insulator using a microscopic continuum model. Strong coupling between the two materials renders the surface state of TI a less useful concept for this problem. Our focus has been on the various modifications to superconductivity by the presence of TI. These include the suppression of the order parameter, the formation of interface modes below the bulk superconducting gap, and the induction of triplet pairing correlations. It is gratifying to see the Fu-Kane effective model emerges in the low energy sector albeit with a set of renormalized parameters. Our results are complementary to previous theoretical work on the proximity effect [**f-k**, **stan**] and confirm the validity of the Fu-Kane model.

We made a few simplifying assumptions in our calculation. The superconductor is described by a two-band model with the valence band well below the Fermi level. Since only electrons near the Fermi surface are relevant for weak coupling superconductivity, we believe our main results are general. As idealizations, the chemical